Scientific/Technical/Management

1 Introduction

Among the key observational properties of main sequence stars in our galaxy, age is the most difficult to determine. Traditionally, fitting isochrones to cluster stars was one of the only precise methods for measuring ages, and was impossible for the majority of isolated field stars. Methods such as asteroseismology and measuring Li abundances require time intensive observations for each target and are not capable of producing the large quantity of ages needed for exoplanet and galactic population studies. To improve our understanding of star and planet formation and evolution, as well as the history of the Milky Way, we must be able to constrain the ages of low-mass stars like the Sun in the galactic field.

Fortunately nature has provided a power means to determine ages for main sequence stars via their rotation. Angular momentum is carried away though magnetically driven stellar winds, which slows the star's rotation over cosmic time. This rotation-based "clock" is known as *gyrochronology*. Cool spots on the star's surface rotate in-to and out-of view, creating small amplitude ($\sim$1%) quasi-periodic changes in the stellar brightness. While rotation periods have previously been laboriously measured from starspot-induced flux modulations for hundreds of stars, space-based photometric surveys have opened the door to homogeneous ensemble measures of stellar rotation, and therefore age. **With the precise, long-duration light curves available from the *Kepler*/K2 mission, we can determine the rotation periods and ages for nearly 100,000 main sequence field stars.**

The *Kepler* mission broke new ground by producing rotation periods for tens-of-thousands of field stars within a single $\sim$110 sq deg field of view, and discovered a surprising bimodal distribution of rotation periods. Two competing explanations have arisen for this mysterious feature: a bimodal age distribution for nearby stars, or a new subtlety in stellar angular-momentum-loss mechanisms. Detailed calibrations of gyrochronology models with the *Kepler* rotation sample also revealed the need for samples of stars with a wider range of ages and compositions. Fortunately the ongoing *Kepler* extended mission, K2, has currently produced light curves from 14 additional fields throughout the Galaxy.

To enable studies of stellar ages from rotation periods with K2, we propose to:

1. Measure accurate rotation periods for every available K2 target, using new statistical methods we have developed to cope with significant instrumental systematics in the K2 data. This value-added dataset will improve the *Kepler* data legacy for field stars, and provide a critical training set for the TESS mission.

2. Produce updated gyrochronology relations based on a wider range of field star ages, and additional open clusters within the K2 fields.

3. Determine the origin of the mysterious rotation period bimodality discoverd with *Kepler* by tracing the rotation period distribution in each K2 field, and out to further distances utilizing public Gaia data.

4. Measure the star formation history within each K2 field using a new Bayesian age-dating system.

2 Scientific Motivation

Galactic archaeology and exoplanet populations are two rapidly accelerating fields of interest within astronomy. Although seemingly unconnected, these two fields are linked by a mutual requirement for precise stellar parameters. To galactic archaeologists, ages and elemental abundances are the most important parameters. Indeed, most galactic archaeology surveys target exactly these properties. For exoplaneteers, masses and radii have historically been the most important stellar parameters for understanding planetary systems. With a growing number of planet hosts with precise masses and radii, attention is turning toward other parameters such as ages to under the history and evolution of these systems. Age is therefore a fundamental stellar parameter of great interest to two large communities of astronomers. However it is a difficult attribute to measure for main sequence F, G, K, and M stars in the field, in part because low-mass dwarfs do not move far on the Color-Magnitude diagram (CMD) during their hydrogen burning lifetimes. Further, competing stellar evolution models predict different ages for the same star. Of all the measurable properties for a large numbers of stars, rotation periods contain the most information about stellar age, and provide the best leverage for advancing our knowledge of galactic archeology as well as exoplanet population demographics.

2.1 Age-Dating Field Stars with Rotation

The seminal work of Skumanich (1972) laid the foundation for our model of the stellar age–rotation–activity relationship. When stars settle onto the main sequence they may have a range of initial rotation periods based on the angular momentum available in their primordial environment. However, rotation velocities converge by a few 100 Myr (for Solar-type stars), and then follow a standard spin-down evolution (Barnes, 2010). Stars continuously lose angular momentum due to magnetically driven winds. Stellar rotation also drives the internal magnetic dynamo, resulting in decreasing surface magnetic activity as the star slows (rotation period increases). Older, slower rotating stars therefore have smaller starspots, making the detection rotation more difficult as stars age. Deriving ages for field stars therefore requires knowing their color (as a proxy for stellar temperature or mass) and their surface rotation period (Barnes, 2007), and can produce ages with errors as low as $\sim$10% (Barnes, 2010).

The rate of this angular momentum loss has historically been calibrated using main sequence stars at a range of masses in stellar clusters with known ages, leading to a useful clock called "gyrochronology" (Barnes, 2003). Several gyrochronology model (or gyrochrones) parameterizations exist, each using various age benchmarks for calibration. Nearly all gyrochronology models suffer from lack of constraint at older ages; often the Sun is the only benchmark used older than $\sim$1 Gyr since accessible nearby open clusters are typically young (< 600 Myr).

In Figure 1 we demonstrate the subtle differences between competing gyrochronology models for Solar mass stars. To increase the available sample of calibration sources available at Gyr ages, Co-I Angus has produced improved gyrochronology models using *Kepler* asteroseismic targets (Angus et al., 2015). Note: the additional calibration sources at Solar

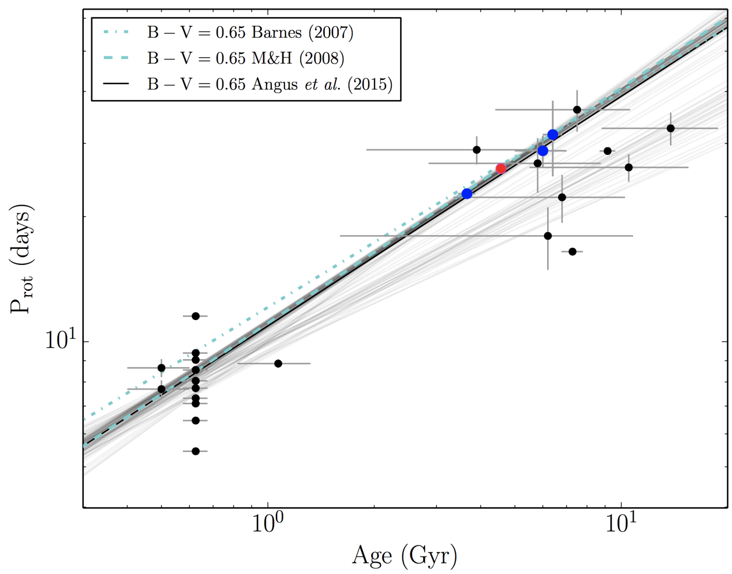

Figure 1: Figure 6 from Angus et al. (2015), showing an improved gyrochronology relation calibrated using *Kepler* asteroseismic targets (black dots) and the Sun (red dot), compared with other standard gyrochronology models (blue dashed and dotted lines).

ages means the Angus model is not forced to exactly fit the Sun's rotation period, as other traditional models do. Unfortunately, asteroseismology cannot yet provide ages for stars with masses much lower than the Sun. *Kepler* rotation period samples have demonstrated that magnetic braking may become less efficient at older ages (van Saders et al., 2016). The Angus et al. (2015) gyrochronology study also found that cluster and asterosismic field star targets may not follow the same spin-down model, possibly indicating bias in the dynamical histories of these samples. Additional calibration sources are desperately needed for stars older than the Sun, and for lower-mass dwarfs.

2.2 Rotation Periods from *Kepler* and K2

Previous ground-based efforts to constrain stellar rotation periods for single, isolated field stars have resulted in few measurements. Detecting rotation from Doppler line broadening requires obtaining medium- to high-resolution spectroscopy of individual targets, and can be subject systematic effects such as from limb darkening approximations (Collins & Truax, 1995). These observations also require time on larger aperture telescopes to reach fainter magnitudes needed to study rotation from low-mass field stars, or for studying the entire mass range within stellar clusters. Ground-based photometric wide-field surveys overcome many of the difficulties in gather large samples of field stars or entire stellar clusters. However, long duration monitoring with relatively high cadence and high photometric precision is required to detect the small amplitude and slowly varying flux modulations from starspots. These campaigns typically yielded rotation samples of hundreds to ∼1000 stars (e.g. Hartman et al., 2010, 2011)

Space-based photometry surveys designed for exoplanet transit searches such as *Kepler* (Borucki et al., 2010) have produced a revolution in stellar rotation studies. The original *Kepler* mission produced light curves up to four years in duration with ∼100 ppm precision at 30-minute cadence for more than 200,000 stars. From this remarkable dataset, more than 30,000 unique stellar rotation periods have been measured using a variety of time series analysis techniques such as the Lomb-Scargle Periodogram (Reinhold et al., 2013) and the Autocorrelation Function (McQuillan et al., 2014). This bounty of rotation periods has also allowed the first ensemble investigations in to stellar surface differential rotation (e.g. Reinhold et al., 2013), revealed stars with near solid-body rotation (Davenport et al., 2015), and highlighted the many degeneracies in disentangling starspot evolution and differential rotation (Aigrain et al., 2015).

After hardware failures made observations of the original field impossible, an extended *Kepler* mission was designed to observe many fields with ∼3 month durations. The K2 mission has observed fields spaced along the ecliptic plane, ranging from low galactic latitudes that include multiple open clusters, to high galactic latitudes that include many older field stars (Howell et al., 2014). The K2 fields also include several benchmark stellar clusters including the Solar-age M67, the Pleiades and Hyades, and M35. To date K2 has released data from 10 distinct campaigns (or fields), including more than 204,000 targets. An additional 4 campaigns are underway with ∼94,000 targets announced, and 2 campaigns pending scheduling. In total, the K2 sample may yield over 350,000 light curves, far exceeding the original *Kepler* mission. Importantly, K2 data quality has been demonstrated to approach that of the original *Kepler* mission (Luger et al., 2016), and has been successfully used to measure rotation periods for select targets such as open cluster stars (e.g. Douglas et al., 2017).

K2 provides the ideal dataset to both extend the *Kepler* studies of field star age distributions, and to amass a sample of better calibration sources for gyrochronology models. The range of K2 fields positions within the Galaxy means the sample spans a much wider variety of stellar ages for more distant stars ($\gtrsim$1pc), and provides multiple opportunities to constrain the local star formation history for nearby stars. This makes the gyrochronology study of field stars with K2 an unique and valuable comparison to complimentary efforts in studying galactic archeology using chemical abundances, such as with APOGEE (Hayden et al., 2014). Producing rotation periods for these older stars, and the additional open clusters including the benchmark Solar age M67 available in the K2 data, will also lead to new gyrochronology relations, and to test the universality of the age–rotation–activity relation put into question by Angus et al. (2015).

2.3 A Mysterious Period Bimodality

One of the most remarkable results from the *Kepler* rotation period catalog was the discovery of a bimodal period distribution among field stars by McQuillan et al. (2013), and is shown in Figure 2a. While a separate sequence of rapid of rotation periods had been known in young stellar clusters due to lower-mass stars settling on to the angular momentum main sequence slower (e.g. Barnes, 2007), this new bimodality was detected from M dwarfs ($T_{eff} \lesssim 4000$), and separated stars at a period of $\sim$20 days. Follow-up analysis of the *Kepler* data by McQuillan et al. (2014) found the period bimodality extended to include K dwarfs. **Recently, PI Davenport discovered this period bimodality extends throughout all masses in the *Kepler* rotation sample for nearby stars, as shown in Figure 2b (Davenport, 2017).**

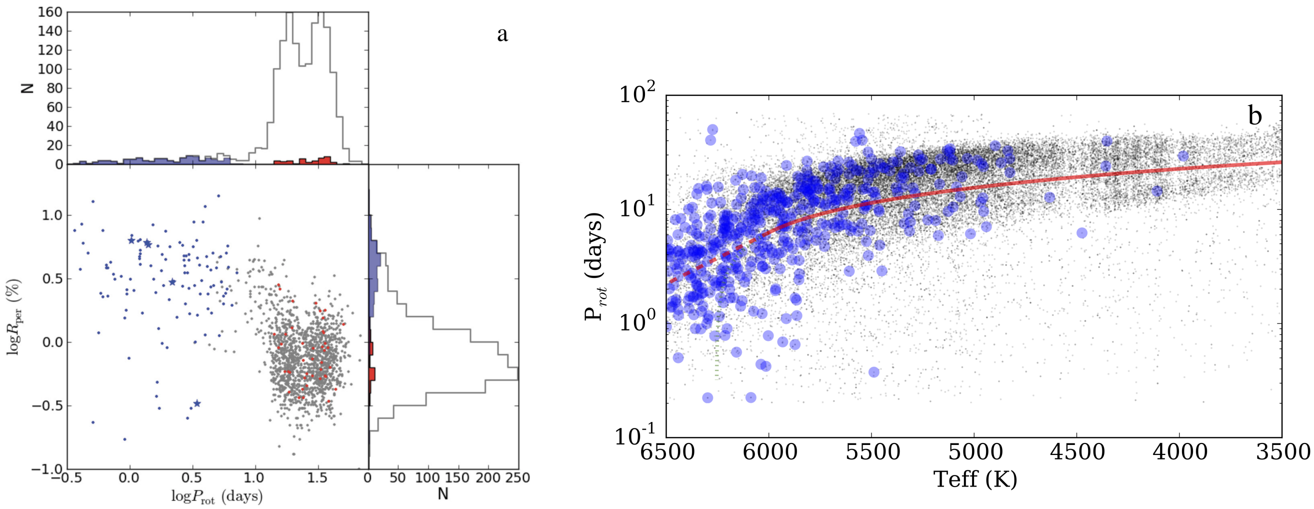

Figure 2: Left – Figure 9 from McQuillan et al. (2013); the discovery of a bimodality in rotation periods from *Kepler* M dwarfs (middle panel). Right – Figure 3 from Davenport (2017), showing all *Kepler* rotation periods from McQuillan et al. (2014) (black dots), and main sequence stars with Gaia DR1 distances (blue circles). The bimodality discovered for M dwarfs extends to nearby G and K stars, and straddles a 600 Myr "gyrochrone" (red line).

Two formation scenarios have been proposed to explain the observed period bimodality. The first scenario, initially proposed by McQuillan et al. (2013), is the rotation period distribution reflects the local star formation history, and thus the bimodality represents a drop in the star formation rate around 600 Myr ago. This model is supported by both the extension of the bimodality to earlier spectral types by Davenport (2017), and also the tentative detection that the two rotation period populations have distinct proper motion distributions. However, such a variation in the star formation rate on short timescales has some tension with independent observational efforts to determine the local star formation history. While Color–Magnitude diagram inversions from Hipparcos have suggested a similarly short timescale variation in star formation of $\sim$0.5 Gyr (Hernandez et al., 2000), other studies find slower variations over several Gyr (e.g. Cignoni et al., 2006). Using white dwarf cooling models to infer the local formation history ("cosmochronology") also supports higher star formation several Gyr ago, but can rarely achieve age resolution better than $\sim$1 Gyr due to small sample sizes (Tremblay et al., 2014). The spatial extent of such coherent and localized variations in star formation history is unknown.

The second scenario to explain this feature is that the period bimodality occurs due to a previously unknown variation in the spin-down evolution for low-mass stars. In this scenario the star formation history would be continuous over the past $\sim$1 Gyr, and around 600 Myr stars would move quickly through the observed period minima due to this unknown phase transition or feedback mechanism. While this model is not currently predicted by angular momentum loss simulations, such rapid transition points in the angular momentum evolution are observed in young clusters. Stars move quickly from the rapidly rotating "convective" sequence (periods of $\lesssim 1$ day) to the "interface" sequence (periods of several days) during the first few hundred Myr, with lower mass stars taking longer to make this transition as they settle onto the main sequence (Barnes, 2003).

The K2 rotation period sample provides the ideal dataset to test these two formation scenarios. If the bimodality is due to an age distribution we would expect to only see the feature locally, and that it would disappear at further distances or along different lines of sight where small scale variations in the star formation history are less apparent. The kinematic separation between the two rotation period populations would be reinforced by supplemental measurements from the upcoming public Gaia data releases. However, if the bimodality is truly due to a transition point in the spin-down evolution at young ages, we would expect to find no little to no variation in this feature as seen in Figure 2b with galactic position or between K2 fields.

3 Proposed Research

3.1 Measuring Rotation periods

We propose the first systematic study of stellar rotation periods from the K2 data. This will include the nearly 300,000 light curves from Campaigns 0-14.

Part of our study will be to assess the qualities of the various data reduction pipelines available for K2 light curves. Each detrending algorithm uses a slightly different approach and will almost certainly provide light curves that differ enough to produce a number of discrepant rotation periods. We will compare the performance of three pipelines in particular: the Vanderburg et al. (2015) light curves, the `everest` Luger et al. (2016) light curves, and the `K2SC` Aigrain et al. (2016) light curves. By visually examining the light curves and Lomb-Scargle periodograms of a number of targets in common between the detrending methods, we will ascertain which pipeline best preserves signal on long timescales. All three of these pipelines are optimized for planet search, however the Aigrain et al. (2016) light curves are designed to preserve stellar variability as much as possible. We expect to find that these light curves preserve rotation signals on the longest timescales.

Once establishing the best detrending method for preserving stellar variability, we will download all the available light curves and, if necessary, run the pipeline on any outstanding targets. We will also produce and examine periodograms using the systematics-insensitive periodogram (SIP) (Angus et al., 2015). This method simultaneously fits light curves with a sinusoid and a noise model constructed from 150 principle components derived from a

PCA of the entire set of `K2` light curves for a given campaign. Although developed for asteroseismology, this algorithm may also be applicable to rotation period analysis, however at the longer timescales of variation produced by stellar rotation, it is likely that the results will suffer from overfitting.

We will use a combination of Lomb-Scargle and autocorrelation function techniques to produce a quick catalogue for early analysis. Although both of these methods are sensitive to noise and can produce spurious rotation period measurements, there relative speed will allow us to rapidly begin initial analysis of the results. We will then apply a procedure for obtaining more accurate and precise rotation periods using probabilistic inference. Co-I Angus recently developed a method for rotation period inference using a Gaussian Process (GP) to model the light curve in the time-domain, rather than extracting periodic signals in the frequency domain Angus et al. (2016a). This GP method produces slightly more precise and accurate rotation periods with more representative uncertainties than Lomb-Scargle and autocorrelation methods. The disadvantage of this GP regression based method is that it can be computationally expensive. However, with the recently developed method for fast Gaussian process inference, `celerite` (Foreman-Mackey et al., 2017), even performing MCMC with the thousands of data points in a `K2` light curve may only take a few minutes. The advantage of computing probabilistic rotation periods is that one can bypass the need to calculate a rotation period at all and simply infer the parameters of stellar populations directly from the light curves themselves. In other words, one can perform hierarchical inference more easily. This may be a level of sophistication that is above and beyond our science goals but it is worth noting that we could take this approach if the data and scientific question warranted it.

Wherever possible we will mask out discontinuous astrophysical signals, such as eclipsing binaries, planet transit or flares that may distort the rotation period signal. We will make use of exoplanet and binary catalogs to identify planet transits and eclipses. We will apply the flare detection algorithm `appaloosa`, built by PI Davenport, to identify and remove flares. It may still be necessary to apply a low-pass filter to the data in order to remove high frequency features that we miss. Fortunately, most of the stellar rotation signals of interest for this study have timescales longer than around a day and will be relatively unaffected by a low-pass filtering algorithm.

The *Kepler* rotation period catalog from McQuillan et al. (2014) found a yield of $\sim 25\%$ of stars had measurable rotation periods using the Autocorrelation Function. From our sample of nearly 300,000 available K2 targets, we expect to recover over 70,000 new periods, bringing the total *Kepler*/K2 sample to $\sim$100,000 stars with measured rotation periods.

We have already measured a number of `K2` rotation periods using an autocorrelation function approach.

3.2 Exploring the Period Bimodality

To determine which formation mechanism gives rise to the bimodal period distribution seen in the original *Kepler* field, we must determine if the feature is only present in nearby stars. However, we must also rule out the unlikely possibility that the bimodality is due to some

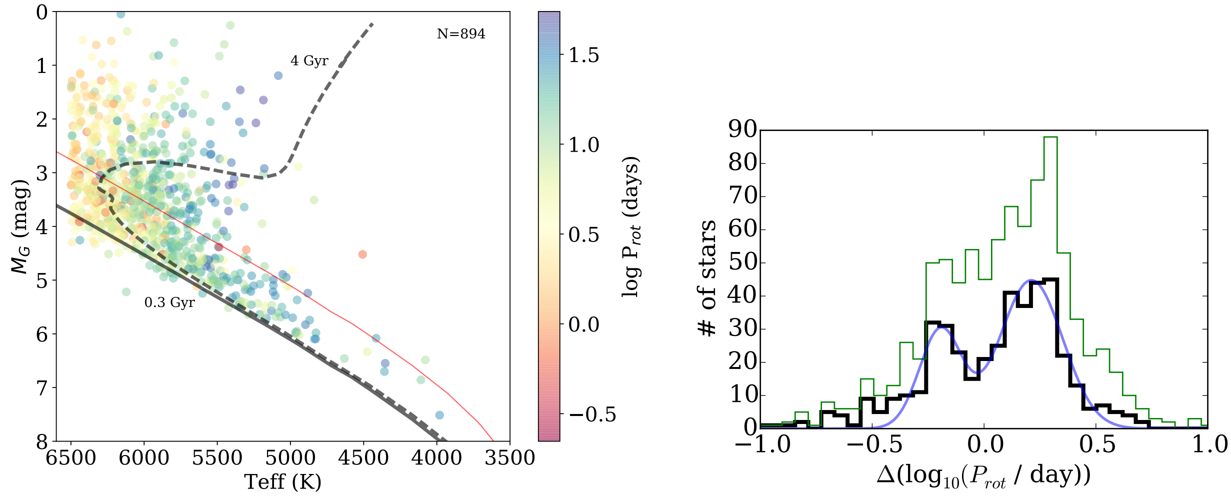

Figure 3: Left – Figure 2 from Davenport (2017), showing the absolute Gaia magnitude versus temperature for *Kepler* stars with known rotation periods in the Gaia DR1 catalog. Sub-giant stars can be separated from main sequence targets using isochrone models (black solid & dashed lines). Right – Figure 4 from Davenport (2017), showing the rotation period distribution relative to a 600 Myr "gyrochrone" before (green line) and after (black line) filtering out sub-giants. The bimodal distribution is apparent, and fit with a 2-Gaussian model (blue line).

systematic error in the *Kepler* data. Within each K2 campaign we will visually inspect the low-mass stars in the color–period space ($T_{eff} < 4500$), as illustrated in Figure 2 for the McQuillan et al. (2013) M dwarf sample. Since these coolest stars are only visible with *Kepler* out to a few hundred pc, this will provide a test of the localization of the bimodality, using a small volume-limited sample. This test provides an important reality check against the period bimodality being due to the processing of the original *Kepler* data itself. Since this initial nearby sample will probe the same close ($\sim$250 pc) volume as in McQuillan et al. (2013) and Davenport (2017), we expect the period bimodality will appear up in most K2 fields for the M dwarfs centered around $P_{rot} = 20$ days.

To reliably map the rotation period distribution as a function of distance we will match our final sample of K2 stars, and the original *Kepler* rotation sample, to the upcoming data release from the Gaia mission (Perryman et al., 2001). With accurate parallaxes from Gaia for all *Kepler* and K2 sources we will also be able to filter out subgiants and binary stars from our sample, leaving only main sequence stars. As Davenport (2017) showed, G dwarfs can only be used to detect the period bimodality if subgiants and binaries are filtered out.Davenport (2017) was able to do this for the *Kepler* rotation period sample using the Gaia DR1 "TGAS" release that included astrometric data for nearby stars (Lindegren et al., 2016), as shown in Figure 3. This reduced the McQuillan et al. (2014) rotation period sample of 33,000 sources down to the 440 brightest main sequence stars within

$\sim$300 pc, roughly the same distance limit reached by the M dwarf-only sample. Studying the period distribution for G dwarfs is critical for including stars at further distances, and therefore sampling different star formation histories. **With the April 2018 data release from Gaia we will be able to study rotation periods for G dwarfs in *Kepler* and K2 out to $\sim$3 kpc.**

Since the K2 campaign fields are spread across the entire ecliptic plane, rotation period data from fields with similar galactic latitudes can be combined to improve the sample size when searching for the bimodality as a function of distance. For example, C1, C3, C10, and C12 are near the North and South Galactic Caps, while C2, C7, and C13 straddle the Galactic Plane. The size scale over which the Milky Way's star formation history varies is unknown. In Andromeda significant variations in star formation histories are seen between 100 pc volumes, as well as large galaxy-wide trends (e.g. Lewis et al., 2015). We will therefore conduct our search for the period bimodality as a function of distance in each *Kepler*/K2 pointing separately, as well in bins of galactic latitude.

We will measure the strength of the bimodal feature by examining the period distribution centered around a 600 Myr gyrochrone, as in Figure 3. By fitting multiple Gaussians to the period distribution in each bin of galactic latitude and distance, we can empirically determine the significance of the bimodality. The Bayesian Information Criterion allows us to analytically determine if one or two (or more) Gaussian curves best represent the rotation distribution in each spatial bin. If the bimodality is due to a localized age distribution of stars, we expect the feature will disappear in this space as we go to further distances and sample different star formation histories. Other period bimodalities may be present, given different star formation histories, but will not align to the 600 Myr gyrochrone. However if the bimodality is a generic feature of angular momentum loss, this two-Gaussian fit from Davenport (2017) will be preferred for every latitude and distance bin.

3.3 Mapping Ages in each Field

Combining our catalog of rotation periods from K2 with the existing rotation catalogs from Kepler will produce the largest set of rotation periods currently available. Using a new technique being developed by CoI Angus, `chronometer`, we will produce an improved age estimate for every star based on rotation values, photometric colors and galactic kinematics from Gaia proper motions. This age map may be used to infer the age distribution of stars across and between K2 fields.

`chronometer` extends isochrone fitting by simultaneously fitting an age-rotation relation and a age-velocity dispersion relation. It combines the information available from these three dating techniques, thus providing more accurate ages than any one of the techniques alone. Of course, this relies on the rotational and kinematic age relations being correct. The age-velocity dispersion relations are relatively well studied and simple. The current picture of the formation history of stars in the Milky Way is that they are formed in the thin disc with relatively small vertical velocities and actions. As time passes these stars encounter more scattering events — close encounters with other stars, and/or interactions with galactic spiral arms. With each of these interactions the star's orbit in the Milky Way is excited.

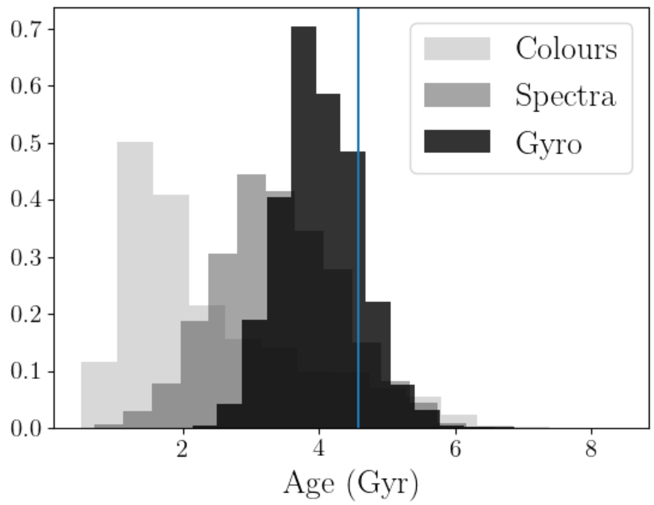

Figure 4: A preliminary demonstration of the power of rotation for age inference, created using `chronometer`. The palest gray histogram shows the probability distribution over ages obtained for the Sun at 10 parsecs using only J, H and K band colors. The darker gray histogram shows the age posterior for the Sun at 10 parsecs using colors and spectroscopic information ($T_{\rm eff}$, $\log(g)$ and $[Fe/H]$). The darkest gray histogram shows the age posterior when colors, spectroscopic information and a rotation period used to infer the age of the Sun at 10 parsecs. This is a preliminary plot with no kinematic information and just three stars. The final model will contain several thousand stars and kinematic information so will be even more powerful than this.

This results in a slow heating of stellar orbits. Old stars reside in the thick disc of the Milky Way — a disc that extends out of the plane of the galaxy. These stars can be identified in Gaia DR1 by converting their proper motions, positions and parallaxes into vertical actions by integrating their orbits in the potential of the Milky Way. Larger vertical actions (larger angular momenta in the vertical direction) correspond to older stars. Truely the *dispersion* in vertical action is a much better tracer of age than vertical action itself.

We combine the following dating methods: gyrochronology, isochrone fitting, asteroseismology and galactic kinematics into one model. In classical isochrone fitting, one might calculate the probability of age A, mass M, $[Fe/H]$, distance D and extinction A_v, given a set of apparent magnitudes in different filters, *e.g.* M_V, M_J and M_K. This can be written

$$\begin{aligned} & p(A, M, [Fe/H], D, A_v | M_V, M_J, M_K) \qquad (1) \\ \propto \quad & p(M_v, M_J, M_K | A, M, [Fe/H], D, A_v) \\ & p(A)p(M)p([Fe/H])p(D)p(A_v). \end{aligned}$$

There are no free parameters in the model here — the model is entirely determined by physics and does not need to be calibrated further. Similarly, in classical gyrochronology, one might calculate the probability of age given rotation period and $B-V$ colour,

$$p(A|P_{rot}, B-V) \propto p(P_{rot}, B-V|A)p(A) \tag{2}$$

In a gyrochronology model however our understanding of the physics is incomplete and some free parameters must be calibrated. In the Barnes (2003) gyrochronology parameterisation, $A = P_{\mathrm{rot}}^{1/n} - (B-V-0.4)^{b/n}$, these free parameters are a, b and n. During a calibration exercise, the observables, A, P_{rot} and $B-V$ will be known and the parameters, a, b and n will be inferred,

$$p(a, b, n|\{A\}, \{P_{rot}\}, \{B-V\}) \propto \{p(A\}, \{P_{rot}\}, \{B-V\}|a, b, n)p(a)p(b)p(n). \tag{3}$$

The vertical action-age relation, $A = \alpha(\sigma_{Jz}^2)^\beta$, also has free parameters that must be calibrated using observations. These free parameters, α and β can again be calibrated via

$$p(\alpha, \beta|\{A\}, \{J_z\}) \propto p(\{A\}, \{J_z\}|\alpha, \beta)p(\alpha, \beta). \tag{4}$$

The unique aspect of our analysis is to combine inference over ages with calibration of the free parameters in the gyrochronology and vertical action-age relations:

$$\begin{aligned} & p(\{A\}, \{M\}, \{[Fe/H]\}, \{D\}, \{A_v\}, a, b, n, \alpha, \beta|\{M_V\}, \{M_J\}, \{M_K\}, \{P_{rot}\}, \{B-V\}, \{J_z\}) \\ \propto\; & p(\{M_v\}, \{M_J\}, \{M_K\}, \{P_{rot}\}, \{B-V\}, \{J_z\}|\{A\}, \{M\}, \{[Fe/H]\}, \{D\}, \{A_v\}, a, b, n, \alpha, \beta) \\ & p(A, M, [Fe/H], D, A_v, a, b, n, \alpha, \beta). \end{aligned} \tag{5}$$

We can use conditional independence to break this down further into the following:

$$\begin{aligned} & p(\{A\}, \{M\}, \{[Fe/H]\}, \{D\}, \{A_v\}, a, b, n, \alpha, \beta|M_V, M_J, M_K, \{P_{rot}\}, \{B-V\}, \{J_z\}) \\ \propto\; & p(\{M_v\}, \{M_J\}, \{M_K\}|\{A\}, \{M\}, \{[Fe/H]\}, \{D\}, \{A_v\})p(A)p(M)p([Fe/H])p(D)p(A_v) \\ & p(\{P_{rot}\}, \{B-V\}, a, b, n|A)p(a)p(b)p(n) \\ & p(\{J_z\}, \alpha, \beta|\{A\})p(\alpha)p(\beta). \end{aligned} \tag{6}$$

In other words

$$\begin{aligned} & p(\text{Ages \& other parameters}|\text{observables}) && (7) \\ \propto\; & \mathcal{L}_{\text{isochronal age}} \times \mathcal{L}_{\text{gyro age}} \times \mathcal{L}_{\text{kinematic age}} && (8) \\ & \times p(\text{Ages \& other parameters}) && (9) \end{aligned}$$

. We can multiply the likelihoods together by making the assumption that the probabilities are conditionally independent, *i.e.* a gyrochronology age depends only on rotation period and colour, not proper motion, for example.

This is esentially an extension of the period bimodality work (if it's an age effect), but to create a detailed map of the ages of these field stars at a range of galactic latitudes in the 17 pencil-beams available from K2. combining with the periods from Kepler, will be even better. Ultimately we'd like to compare to the age distributions in simulations of these fields from TRILEGAL, and from other age indicators (asteroseismology, flare ages, etc).

4 Team Qualifications

PI Davenport has used *Kepler* to conduct the largest survey to-date of stellar activity from flares, as well as multiple investigations of starspots and their evolution with time using *Kepler* data. From these studies, Davenport has developed an age model for flare activity that will be directly comparable to the ages and starspot amplitudes derived from this study. He also recently discovered the rotation period bimodality first noted with *Kepler* M dwarfs by McQuillan et al. (2013) extends to G and K dwarf stars (Davenport, 2017). Davenport previously collaborated on NASA ADP grant NNX09AC77G to characterize NIR variability using the 2MASS Calibration Scan Point Source Working Database (Davenport et al., 2012, 2015). He has mentored numerous students on projects using *Kepler* data, resulting in student-led publications such as the flare activity of a unique M dwarf binary system GJ 1245AB (Lurie et al., 2015), and exploring the poorly understood origins of wide binary stars through stellar rotation (R. Clarke in prep). He will manage the overall project, detect and remove short period variability from flares in the light curves, and lead the investigation and publication on the nature of the bimodal period distribution.

Co-I Angus is an expert in the extraction of periodic signals from *Kepler* data using Gaussian Processes (Angus et al., 2016a) and other cutting-edge statistical techniques. She is the author of tools for generating Systematics-Insensitive Periodograms for both *Kepler* and K2 data (Angus et al., 2016b), as well as new gyrochronology calibrations using *Kepler* asteroseismic targets (Angus et al., 2015). She will lead the effort to measure and publish rotation periods for all K2 sources, and guide students in measuring ages for field stars.

Covey

Kipping

Agueros

5 Relevance to NASA Programs

history of MWY, age of planet systems, TESS

6 Plan of Work

Year 1: process all rotation period data
Year 2: write papers

References

Aigrain, S., Parviainen, H., & Pope, B. J. S. 2016, MNRAS, 459, 2408

Aigrain, S., Llama, J., Ceillier, T., et al. 2015, MNRAS, 450, 3211

Angus, R., Aigrain, S., & Foreman-Mackey, D. 2016a, IAU Focus Meeting, 29, 191

Angus, R., Aigrain, S., Foreman-Mackey, D., & McQuillan, A. 2015, MNRAS, 450, 1787

Angus, R., Foreman-Mackey, D., & Johnson, J. A. 2016b, ApJ, 818, 109

Barnes, S. A. 2003, ApJ, 586, 464

—. 2007, ApJ, 669, 1167

—. 2010, ApJ, 722, 222

Borucki, W. J., Koch, D., Basri, G., et al. 2010, Science, 327, 977

Cignoni, M., Degl'Innocenti, S., Prada Moroni, P. G., & Shore, S. N. 2006, A&A, 459, 783

Collins, II, G. W., & Truax, R. J. 1995, ApJ, 439, 860

Davenport, J. R. A. 2017, ApJ, 835, 16

Davenport, J. R. A., Becker, A. C., Kowalski, A. F., et al. 2012, ApJ, 748, 58

Davenport, J. R. A., Ruan, J. J., Becker, A. C., Macleod, C. L., & Cutri, R. M. 2015, ApJ, 803, 2

Douglas, S. T., Agüeros, M. A., Covey, K. R., & Kraus, A. L. 2017, ArXiv e-prints, arXiv:1704.04507

Foreman-Mackey, D., Agol, E., Angus, R., & Ambikasaran, S. 2017, ArXiv e-prints, arXiv:1703.09710

Hartman, J. D., Bakos, G. Á., Kovács, G., & Noyes, R. W. 2010, ArXiv e-prints, arXiv:1006.0950

Hartman, J. D., Bakos, G. Á., Noyes, R. W., et al. 2011, AJ, 141, 166

Hayden, M. R., Holtzman, J. A., Bovy, J., et al. 2014, AJ, 147, 116

Hernandez, X., Valls-Gabaud, D., & Gilmore, G. 2000, MNRAS, 316, 605

Howell, S. B., Sobeck, C., Haas, M., et al. 2014, PASP, 126, 398

Lewis, A. R., Dolphin, A. E., Dalcanton, J. J., et al. 2015, ApJ, 805, 183

Lindegren, L., Lammers, U., Bastian, U., et al. 2016, A&A, 595, A4

Luger, R., Agol, E., Kruse, E., et al. 2016, AJ, 152, 100

Lurie, J. C., Davenport, J. R. A., Hawley, S. L., et al. 2015, ApJ, 800, 95

McQuillan, A., Aigrain, S., & Mazeh, T. 2013, MNRAS, 432, 1203

McQuillan, A., Mazeh, T., & Aigrain, S. 2014, ApJS, 211, 24

Perryman, M. A. C., de Boer, K. S., Gilmore, G., et al. 2001, A&A, 369, 339

Reinhold, T., Reiners, A., & Basri, G. 2013, A&A, 560, A4

Skumanich, A. 1972, ApJ, 171, 565

Tremblay, P.-E., Kalirai, J. S., Soderblom, D. R., Cignoni, M., & Cummings, J. 2014, ApJ, 791, 92

van Saders, J. L., Ceillier, T., Metcalfe, T. S., et al. 2016, Nature, 529, 181

Vanderburg, A., Johnson, J. A., Rappaport, S., et al. 2015, Nature, 526, 546